Published in final edited form as:
J Immunol. 2012 February 1; 188(3): 1381–1393. doi:10.4049/jimmunol.1102359.

Localized Production of IL-10 Suppresses Early Inflammatory Cell Infiltration and Subsequent Development of IFN-γ-Mediated Lyme Arthritis[1]

F. Lynn Sonderegger[*], **Ying Ma**[*], **Heather Maylor-Hagan**[*], **James Brewster**[*], **Xiaosong Huang**[*], **Gerald J. Spangrude**[*,†], **James F. Zachary**[‡], **John H. Weis**[*], and **Janis J. Weis**[2,*]

[*]Department of Pathology, Division of Microbiology and Immunology, University of Utah, Salt Lake City, UT 84112

[†]Department of Medicine, Division of Hematology, University of Utah, Salt Lake City, UT 84112

[‡]University of Illinois at Urbana-Champaign, Urbana, Illinois, 61802

Abstract

IL-10 is a non-redundant inflammatory modulator that suppresses arthritis development in *Borrelia burgdorferi* infected mice. Infected B6 IL-10$^{-/-}$ mice were previously found to have a prolonged interferon-inducible response in joint tissue. Infection of B6 IL-10 reporter mice identified macrophages and CD4^{+} T cells as the primary sources of IL-10 in the infected joint tissue, suggesting that early local production of IL-10 dampened the pro-arthritic interferon response. Treatment of B6 IL-10$^{-/-}$ mice with anti-IFN-γ reduced the increase in arthritis severity and suppressed interferon-inducible transcripts to wild type levels, thereby linking dysregulation of IFN-γ to disease in the B6 IL-10$^{-/-}$ mouse. Arthritis in B6 IL-10$^{-/-}$ mice was associated with elevated numbers of NK cell, NKT cell, α/β T cell, and macrophage infiltration of the infected joint. FACS lineage sorting revealed NK cells and CD4^{+} T cells as sources of IFN-γ in the joint tissue of B6 IL-10$^{-/-}$ mice. These findings suggest the presence of a positive feedback loop in the joint tissue of infected B6 IL-10$^{-/-}$ mice, where production of inflammatory chemokines, infiltration of IFN-γ producing cells, and additional production of inflammatory cytokines result in arthritis. This mechanism of arthritis is in contrast to that seen in C3H mice, where arthritis development is linked to transient production of Type I interferon, and develops independently of IFN-γ. Due to the sustained interferon response driven by NK cells and T cells, we propose the B6 IL-10$^{-/-}$ mouse as a potential model to study the persistent arthritis observed in some human Lyme disease patients.

Introduction

Lyme disease is the manifestation of one or more lesions that result following infection with the spirochete *Borrelia burgdorferi* (1), which is transmitted to humans and animals through the bite of infected *Ixodes* ticks (2–4). These bacteria establish infections of skin, cardiac, nervous, and/or connective tissue of the joint (5), and can cause disease at these sites (4). Lyme arthritis occurs in up to 60% of infected humans not treated early with antibiotics, and may develop months after the initial infection (6). This arthritis is characterized by swelling, edema and a moderate inflammatory infiltrate that consists primarily of granulocytes (7).

[1]This work was supported by Public Health Services grants AI-32223 and AI-43521 to J.J.W., AI-24158 and AI-088451 to J.H.W., and the Training Program in Microbial Pathogenesis 5T32-AI-055434.

[2]Address correspondence and reprint requests to Dr. Janis J. Weis, Department of Pathology, University of Utah, 15 North Medical Drive East, Room 2100, Salt Lake City, UT 84112-5650. janis.weis@path.utah.edu.

Arthritis can be recurrent if untreated (6–8). Most human patients with Lyme arthritis respond to antibiotic therapy, after which the arthritis eventually resolves (5). However, in some cases arthritis persists after treatment designed to eradicate infection suggesting that there is a subset of individuals that maintain a long-term inflammatory response in the absence of active infection (5, 9).

The acute, infection-associated arthritis seen in humans has been modeled using inbred mice, in particular, the C3H/He (C3H) and C57BL/6 (B6) strains. In mice infected intradermally, *B. burgdorferi* reach maximal numbers in the joint tissue at 2 weeks post infection, and arthritis severity peaks at 4 weeks after infection (10–12). Genetic susceptibility to arthritis development is clearly illustrated in inbred mice, and is independent of spirochete numbers in the joint (11, 13, 14). In C3H mice, arthritis is severe, with robust infiltration of neutrophils along with the accumulation of edema, as well as proliferation of synoviocytes of the tibiotarsal tendon sheath (10, 13). These lesions have also been observed in B6 mice, but the severity of disease is greatly decreased in comparison (11, 13). Severe arthritis development in C3H mice has not consistently been linked to skewing of T cell responses, such as IFN-γ-producing T_H1 cells (15–17), or a lack of T_H2 responses (18, 19), and in fact, studies using C3H *scid* mice demonstrated that T and B lymphocytes were not required for severe arthritis in C3H mouse line (20). Rather than a T cell driven disease, arthritis in C3H mice has been linked to the production of Type I interferon (21), MMP-9 (22), and chemokines that signal through CXCR2 (23), and is also regulated through the CD14 pathway (24).

Much insight has been gained from the C3H mouse models of Lyme arthritis, as these mice have a robust phenotype that accurately mimics many signs associated with Lyme borreliosis in humans. However, the C3H mouse does not completely model the spectrum of pathology observed in human Lyme arthritis (6). The apparent lack of T cell involvement in this mouse model appears contradictory to what is reported in some human patients (25), where both T_H1 (26) and γ/δ (27, 28) T cells have been implicated. Indeed, this holds true for a select group of Lyme arthritis patients who experience persistent arthritis after appropriate antibiotic therapy. It has been hypothesized that this persistent arthritis is due to one or more of the following: 1) autoimmunity, 2) persistent undetectable levels of infection, 3) persistence of bacterial antigens, or 4) dysregulated inflammatory responses (1). Recent findings from Shin *et al* demonstrated a possible dysregulated inflammatory response in patients with antibiotic-refractory arthritis, as synovial fluid from these individuals contained elevated concentrations of the cytokines IL-1β, IL-6, IFN-γ, and others, as well as extremely high concentrations of the chemokines *CXCL9* and *CXCL10* (9).

The C57BL/6 (B6) mouse model is a useful tool in the study of Lyme arthritis, as it is resistant to the development of severe disease. Multiple gene-targeted knockouts are available on this background, and thus, the B6 model provides an opportunity to explore specific deficiencies of acute and chronic inflammatory responses and mediators that may exacerbate Lyme arthritis (29–35). IL-10 deficiency in B6 mice is one such knockout model, and this deficiency results in increased arthritis severity, even with 5–10 fold fewer spirochetes in the joint tissues of infected mice than observed in B6 mice (36). Infection of B6 IL-$10^{-/-}$ mice with a related spirochete, *Borrelia turicatae* also leads to increased disease severity but enhanced control of the pathogen (37). Production of pro-inflammatory cytokines by murine immune cells stimulated with *B. burgdorferi* is regulated by IL-10 (38), and in fact, previous microarray analyses of infected joint tissue from B6 IL-$10^{-/-}$ mice revealed a sustained induction of the cytokines *IL-1β*, *IL-6*, and *IFN-γ* and chemokines *CXCL9*, and *CXCL10* (39). None of these pro-inflammatory transcripts showed signs of resolution, as they all had increased expression at 4 weeks of infection compared to earlier measurements. In fact, the most highly induced gene in B6 IL-$10^{-/-}$ mice, *CXCL9*,

displayed >500 and >800 fold induction at 2 and 4 weeks of infection, respectively. These findings are strikingly similar to the cytokine and chemokine profiles observed by Shin *et al*, in the synovial fluid of patients with treatment-refractory Lyme arthritis (9).

In the current study, we have extended our analysis of the B6 IL-$10^{-/-}$ mouse as a Lyme arthritis model resulting from a dysregulated inflammatory response to low levels of joint spirochetes. We identify the pro-inflammatory cytokine IFN-γ as a primary target of IL-10 in the joint tissue of the normally arthritis resistant B6 mice, and determine that macrophages and $CD4^+$ T cells in infected joint tissue are the primary sources of this regulatory cytokine. Furthermore, we identify both NK cells and $CD4^+$ T cells as the primary sources of IFN-γ in the infected joints of B6 IL-$10^{-/-}$ mice. We propose that disruptions of the delicate balance between pro and anti-inflammatory signaling in both innate and adaptive immunity result in unique patterns of lesions during *B. burgdorferi* infection of joint tissue. Furthermore, the B6 IL-$10^{-/-}$ mouse provides an opportunity to dissect inflammatory events that are normally highly regulated, and result in increased disease severity when this balance is disrupted.

Materials and Methods

Mice, infections, and assessment of arthritis severity

C57BL/6 (B6) wildtype, B6.129P2-*IL-10tm1Cgn*/J (B6 IL-$10^{-/-}$), (B6.129S6-*Il10*^{tm1Flv}/J (*tiger)*, mice were purchased from The Jackson Laboratories. B6-LY5.2/Cr ($Ly5.1^+$) congenic mice were purchased from NCI. All mice were housed in the University of Utah Animal Research Center (Salt Lake City, UT) and strict adherence to institutional guidelines were followed. To avoid colitis development, B6 IL-$10^{-/-}$ mice were kept on antibiotic water (trimethoprim and sulfamethoxazole) until one day prior to infection. Mice were infected with 2×10^4 bacteria of the clonal *Borrelia burgdorferi* strain N40 intradermally into the skin of the back. Ankle measurements were obtained using a metric caliper before and at 4 weeks of infection. Joint tissue was prepared for assessment of histopathology as described (36). Briefly, after removal of skin, rear ankle joints were fixed in 10% neutral buffered formalin. After decalcification, joints were embedded in paraffin, and 5μm sections were stained with hematoxylin and eosin. Each slide was scored from 1 to 5 for various aspects of disease, including neutrophil and mononuclear infiltration, tendon sheath thickening, and reactive/reparative responses, with 5 representing the most severe lesion, and 0 representing no lesion. Ankle measurements and histopathology were assessed in a blinded fashion. Infection was confirmed in mice sacrificed prior to 14 days of infection by culturing bladder tissue in BSK II media containing 6% rabbit serum, phosphamycin, and rifampicin. ELISA quantification of *B. burgdorferi*-specific IgM and IgG concentrations were used to confirm infection in mice euthanized at and after 14 days of infection as described (11, 34).

Preparation of single cell suspensions from mouse tissue

Single cell suspensions were prepared from rear ankle joint tissue as described previously (21), with a few modifications. After excision, joints were placed into Petri dishes containing 3 ml digestion buffer. For flow cytometry experiments, the buffer consisted of 1mg/ml collagenase A (Roche), 10mM NaN_3, and 5% NCS in HBSS. For experiments where joint cells were sorted for transcriptional analysis, the buffer consisted of endotoxin-free Liberase TM (Roche) at 0.2 mg/ml in RPMI 1640. Collagenase digestions were incubated for 2 hours at 37° C, while Liberase digestions were incubated for 1 hour at 37° C. After incubation, digestion reactions were filtered through a 100 μm cell strainer, centrifuged, and the red blood cells lysed. Single cell suspensions of lymph nodes were prepared by smashing lymph nodes through a 100μm cell strainer into Petri dishes

containing flow cytometry buffer. Blood was obtained by cheek puncture, and collected in Eppendorf tubes containing acid citrate dextrose (ACD). Blood leukocytes were isolated as described (40).

Flow cytometry

All flow cytometry data was analyzed using BD CellQuest Pro software. Sorting experiments were performed using a BD FACSAria II. All other FACS data were collected on a BD FACS Canto II flow cytometer. 7'AAD (eBioscience) was used in all experiments (excluding samples stained for FoxP3), and dead cells were excluded from analyses, as were doublet cells. At least 10^5 viable, non-doublet events were acquired for each sample. All antibodies used for flow cytometry were purchased from either BioLegend or eBioscience. Unconjugated F_c blocking antibody (clone 93 eBioscience) was included in all antibody-labeling experiments. Fluorochrome-conjugated antibodies used in this study were as follows: FITC conjugated α-CD4 (RM4-4), α-CD8α (53–6.7), α-B220 (RA3-6B2), α-F4/80 (BM8), α-TCR-β (H57-597); PE conjugated α-CD3ε (145-2C11), α-NK1.1 (PK136), α-NKp46 (29A1.4), α-Ly6C (HK1.4), α-F4/80 (BM8), α-FoxP3 (FJK-16s); PE-Cy-7 conjugated α-CD4 (GK1.5), α-CD11b (M1/70), α-TCR-β (H57-597); APC conjugated α-CD3ε (145-2c11), α-CD11c (N418), αCD45.1/Ly5.1 (A20), α-F4/80 (BM8), α-TCR-β (H57-597); Alexa Fluor 700 conjugated α-CD8α (53–6.7), α-Ly6G/Ly6C (RB6-8C5); Pacific Blue conjugated α-CD45.2 (104), α-B220 (RA3-6B2), α-TCR-β (H57-597). The APC-conjugated tetramer mCD1d was obtained through the NIH Tetramer Facility as both unloaded and loaded with the synthetic lipid PBS-57.

Injection of monoclonal antibodies

Antibodies used in neutralization or depletion studies were purchased from Bio X Cell, and were aggregate and endotoxin free, and sterile. Antibodies used were as follows: α-IFN-γ (XMG1.2), α-CD4 (GK1.5), and α-NK1.1 (PK-136). Isotype control antibodies used were: Rat IgG1 (HPRN), Rat IgG2b (LTF-2) termed isotype 2, (Figure 7), and Mouse IgG2a (C1.18) termed isotype 1 (Figure 7). All antibodies were delivered by intra peritoneal injection. For neutralization of IFN-γ, mice were initially injected with 1mg α-IFN-γ or isotype control antibody one day prior to infection. Additional doses of 0.5mg α-IFN-γ or isotype control were administered every 4–5 days. For depletion of $CD4^+$ T cells, mice were injected with 200μg α-CD4, or isotype control antibody, one day prior to, and the day of infection. Depletion was maintained with additional 200μg injections every 5 days. Depletion efficiency was determined to be >95% at time of sacrifice in both the spleen and blood. For depletion of NK cells, mice were injected with 250μg α-NK1.1, or isotype control antibody one day prior to, and the day of infection. Depletion efficiency was 80–90% in the spleen and blood.

Isolation of RNA and quantitative RT-PCR

For all experiments examining gene expression in joint tissue, mice were killed, and the skin was removed from the tibiotarsal joints. Ankle joints were excised, placed in Eppendorf tubes, and frozen immediately in dry ice/ethanol, and stored at −80°C. Isolation of total RNA from joint tissue was performed by acid guanidine extraction as described (41). 5μg joint RNA was reverse-transcribed as described (21). Primers sequences used in this study were: *CXCL10* Forward (5'-GAA ATC ATC CCT GCG AGC CTA TCC-3'), Reverse (5'-GCA ATT AGG ACT AGC CAT CCA CTG GG-3', *F4/80* Forward (5'-TGG GAA AGA CTG GAT TCT GGG-3'), Reverse (5'-GGA GCC ATT CAA GAC AAA GCC-3'); *CD4* Forward (5'-CAA GAA GCA GAG TGA AGG AAG GAC-3'), Reverse (5'-CAG CAG CAG CAG CAA GCG-3'); *CD49b* Forward (5'-ATA AGG AGT GTG GCA GCG ATG G-3'), Reverse (5'-CCC CTC TGT TTT TCA GGA TGA CTG-3'); *IL-10CD* (does not recognize sterile transcript produced by B6 IL-$10^{-/-}$ mouse) Forward (5'-GCT CTT ACT

GAC TGG CAT GA-3'), Reverse (5'-TTC CGA TAA GGC TTG GCA AC-3'. Primer sequences for *β–actin* (39), *CXCL9* (21), *IGTP* (39), *IIGP* (39), and *Vα14-Jα18* iTCR (42) used in this study can be found with their respective citations. All RT-PCR experiments were conducted on a Roche LC-480.

Isolation of DNA and quantification of joint spirochetes

For quantification of joint spirochetes at 4 weeks post infection, total DNA was isolated as described (12). Quantitative PCR was performed on a Roche LC-480. Spirochete quantification was performed by amplification of the *B. burgdorferi recA* gene, followed by normalization to the mouse *nidogen* gene.

Generation of radiation chimeras

B6 IL-10$^{-/-}$ mice 5 weeks of age were lethally irradiated with 2 doses of 525 cGy 3 hours apart using a GE Isovolt Titan. Twenty-four hours post irradiation; splenocytes were harvested from donor mice (either B6 IL-10$^{-/-}$ Ly5.2^{+}, or congenic B6 mice that were Ly5.1^{+}). Irradiated mice were then injected *i.v.* with 2×10^{7} splenocytes in a 200μl volume. Chimerism was determined at 2, 4, 6, and 14 weeks post irradiation by flow cytometry analysis of blood leukocytes. At 6 and 14 weeks of engraftment, B cells and myeloid lineage cells were found to be >90% donor-derived, while T cells were approximately 60% donor-derived. Total blood leukocyte counts were comparable to those from non-irradiated control mice at 6 and 14 weeks post transplantation.

ELISA analysis of serum IFN-γ

Blood was obtained from mice by submandibular puncture at the time of euthanasia. Blood was allowed to clot, centrifuged, and serum was collected, and stored at −20°C prior to analysis. IFN-γ concentration in serum samples were detected by sandwich ELISA using clone R46A2 as the capture antibody, and biotinylated antibody (XMG1.2) for detection.

Data and statistical analyses

All graphical data represent the mean ± SEM. Statistical analysis was performed using Prism 5.0c software. Unless otherwise indicated, data were analyzed by one-way ANOVA with the Bonferoni post-hoc test for pair-wise comparisons. Categorical data for histopathology was assessed by the Mann Whitney U test. Statistical significance is indicated by (*), (**), or (***) with p values of < 0.05, < 0.01, and < 0.001 respectively.

Results

Localized production of arthritis-modulating IL-10 in joint tissue is dependent on infiltrating leukocytes

Previous publications with B6 IL-10$^{-/-}$ mice have established a unique role for IL-10 in modulating the inflammatory response to *B. burgdorferi*, restricting the severity of arthritis while permitting bacterial survival within joint tissue (36, 43). Microarray analyses of infected joint tissue further revealed a prolonged induction of transcripts for IFN-γ and interferon-inducible genes in B6 IL-10$^{-/-}$ mice, in contrast to the transient upregulation observed in infected C3H mice, beginning 2 weeks following infection (39). These findings suggested that suppression of arthritis in B6 mice was dependent on a tissue-localized source of IL-10, possibly acting to suppress local production of IFNγ. As arthritis in B6 mice is more severe in the absence of IL-10, we sought to determine the cellular source(s) of this anti-inflammatory cytokine. For the initial characterization, B6 IL-10$^{-/-}$ mice were lethally irradiated, and served as recipients for Ly5.1^{+} B6 splenocytes, or autologous Ly5.2^{+} B6 IL-10$^{-/-}$ splenocytes in a protocol designed to reconstitute both hematopoietic lineage cells

and hematopoietic stem cells. Mice were infected 12 weeks post irradiation/transplantation and sacrificed 2 weeks later, whereupon expression of *IL-10*, *IFN-γ*, and interferon-inducible gene expression were assessed by RT-PCR. Importantly, expression of *IL-10* in the joint tissue of Ly5.1→ B6 IL-$10^{-/-}$ chimeric mice was equivalent to *IL-10* expression in joint tissue of un-irradiated, infected, B6 mice (Figure 1A), whereas *IL-10* transcripts were not detectable in B6 IL-$10^{-/-}$ mice reconstituted with splenocytes from B6 IL-$10^{-/-}$ mice. Evidence that active IL-10 protein was produced in the joint tissue of Ly5.1→ B6 IL-$10^{-/-}$ chimeras is provided by the resulting suppressed expression of *IFN-γ* and the interferon responsive transcripts *CXCL9* and *CXCL10* to levels found in the joint tissue of infected wild type B6 mice (Figure 1B, C, D). Thus, leukocyte derived IL-10 is sufficient to suppress the interferon-inducible response in the joint tissue of *Borrelia burgdorferi* infected B6 mice.

Both $CD4^+$ T cells and macrophages are sources of IL-10 in the B. burgdorferi-infected

To identify the IL-10-producing cell type(s) infiltrating joint tissues during *B. burgdorferi* infection, an IL-10 reporter mouse in which an IRES-GFP cassette was knocked into the 3' UTR of the *Il10* gene was utilized. The availability of this mouse, designated "*tiger*", on the B6 background allowed direct assessment of the cell types responsible for IL-10 production in response to *B. burgdorferi* by flow cytometry of cells recovered from localized tissue (44). Joint tissue and inguinal lymph nodes were collected from uninfected control mice or from mice at day 14 of infection, the time previously associated with up-regulated levels of *IL-10* in B6 mice (39). Single cell suspensions were prepared from inguinal lymph nodes and from joint tissue disrupted by enzymatic digestion, as described in Materials and Methods, and stained with lineage markers. Lymph node and joint cells from uninfected *tiger* mice or control mice showed little to no GFP^+ cells in either the $CD45^+$ or $CD45^-$ fraction (Figure 2A, i–ii, iv–v), consistent with the observation that *IL-10* expression is extremely low in uninfected mice (Figure 1A). However, initial analysis of both tissues from infected *tiger* mice revealed a small population of IL-10 $(GFP)^+$ cells, all of which also expressed the common leukocyte antigen, CD45.2, (Figure 2A, iii, vi). The observation that all IL-10 $(GFP)^+$ cells were also $CD45.2^+$, is consistent with data obtained with radiation chimeras, which concluded that anti-inflammatory IL-10 is leukocyte-derived (Figure 1A). Further characterization of the IL-10 $(GFP)^+$ cells in the draining lymph nodes of infected *tiger* mice revealed them to also stain as TCR-β^+ and $CD4^+$ (Figure 2B, iii, iv) with very few GFP^+ cells staining positive for NK1.1, CD8α, or B220 (Figure 2B, ii, v, vi). When total IL-10 $(GFP)^+$ lymph node cells were gated, >90% of these cells were double positive for CD4 and TCR-β (Figure 2C), demonstrating that $CD4^+$ T cells are the primary source of IL-10 in the inguinal lymph nodes of *B. burgdorferi* infected mice.

To identify the specific lineages of the $CD45^+$, *IL-10* expressing cells in the joint tissue at 2 weeks of infection, single cell suspensions were prepared from infected joint tissue, and stained with the same lineage markers used to analyze lymph node cells. As previously indicated, 1.39% of joint cells were IL-10 $(GFP)^+$ (Figure 1A, vi). Further analysis of joint cell lineages identified populations of GFP^+ cells that also stained positive for TCR-β and CD4, at a frequency of 0.22% and 0.23% respectively (Figure 2D, iii, iv). As was seen in the infected lymph nodes, IL-10 $(GFP)^+$ cells had little to no staining for NK1.1, CD8α, or B220 (Figure 2D, ii, v, vi). When total IL-10 $(GFP)^+$ joint cells were gated, 19% stained double positive for TCR-β and CD4 (Figure 2E), demonstrating that $CD4^+$ T cells are significant source of IL-10 in the infected joint. Because $CD4^+$ T cells accounted for one fifth of the total *IL-10* expressing cells, a second non-T cell, non-lymphocyte source of IL-10 in the infected joint was suspected. Additional analysis of joint cells from infected *tiger* mice revealed that IL-10 (GFP^+) cells stained positive for CD11b and for the macrophage marker F4/80, both at a frequency of 1.08% (Figure 2F, i, iv), indicating a myeloid source of IL-10.

Very few of the GFP^+ cells were positive for CD11c or Gr-1/Ly6c (Figure 2F, ii, iii), thus neither dendritic cells nor granulocytes are major sources of IL-10 in the joint. When total IL-10 $(GFP)^+$ cells were gated, 80% stained double positive for CD11b and F4/80, identifying these cells as macrophages (Figure 2G), and accounting for the non-T cell source of IL-10 in the infected joint. Together these data indicate that $CD4^+$ T cells are the primary source of IL-10 in the draining lymph nodes of infected B6 mice, while both tissue macrophages and $CD4^+$ T cells produce IL-10 in the joint tissue of *B. burgdorferi* infected mice.

Kinetic analysis of IL-10 expression in joint tissue

The duration and magnitude of *IL-10* expression in response to *B. burgdorferi* infection in the joint tissue was further assessed in *tiger* mice by flow cytometry, at 7, 11, and 14 days of expression. $CD4^+$ T cells were quite rare in joint tissue of uninfected animals and at day 7 post-infection (Figure 3A-i, ii, and 3B). A robust infiltrate of $CD4^+$ T cells was observed, that peaked at day 11 of infection, with 45% of the $CD4^+$ T cells expressing IL-10 (GFP), (Figure 3A iii) and 3B). By day 14 post infection the percentage and total number of infiltrating $CD4^+$ T cells expressing IL-10 (GFP) had dropped to 21% (Figure 3A, iv, 3C). To determine whether regulatory T cells (T_{reg}) were responsible for this IL-10 response, joint cells from day 11 *tiger* mice were also analyzed for the T_{reg} definitive transcription factor, FoxP3. Because, concurrent analysis of IL-10 (GFP) and FoxP3 was not possible due to loss of cytoplasmic GFP from cells treated to allow intranuclear FoxP3 staining, the distributions of GFP^+ and $FoxP3^+$ T cells were assessed. In the day 11 lymph nodes, 12% of the $CD4^+$ T cells were $FoxP3^+$, consistent with other reports that T_{reg} cells account for ~10% of $CD4^+$ T cell population. Only 1–2% of the $CD4^+$ T cells in lymph nodes were IL-10 $(GFP)^+$ (data not shown). In joint tissue at day 11 post infection, only 12% of the $CD4^+$ T cells displayed intracellular staining for FoxP3 (Figure 3D-ii), while 45% of the total infiltrating $CD4^+$T cells expressed IL-10 (GFP) (Figure 3A iii). Thus, the number of IL-10 $(GFP)^+$ $CD4^+$ T cells was significantly greater than the number of $FoxP3^+$ CD4 T cells in the joint tissue (Figure 3E). This observation suggests that the IL-10 producing $CD4^+$ T cells in the joint consist of both T_{reg} and non-T_{reg} cells. As in previous experiments, $CD11b^+$ $F4/80^+$ macrophages constituted a major portion of cells recovered from the joint tissue after collagenase digestion. The maximal infiltration of total and IL-10 (GFP) expressing macrophages into the joint tissue was at day 11 of infection, and levels remained elevated at day 14 (Figure 3F–G). Although both the GFP mean fluorescence intensity (MFI) and frequency of IL-10 (GFP) expression in the total $CD4^+$ T cell population was significantly greater than in the macrophage population at 11 and 14 days of infection (Table I), IL-10 (GFP^+) macrophages in the joint were more plentiful than $CD4^+$ T cells at day 14 post infection (Table I). Thus, on a single cell basis, $CD4^+$ T cells produce more IL-10 than their macrophage counterparts, but as distinct populations, macrophages and CD4+ T cells are comparable in their ability to produce IL-10.

Both Systemic and localized production of IFN-γ is associated with increased arthritis severity in B6 IL-$10^{-/-}$ mice

Previous microarray analysis revealed a sustained up-regulation of IFN-γ and interferon-inducible genes in the joint tissue of infected B6 IL-$10^{-/-}$ mice at 2 and 4 weeks post infection (39). Further analysis of serum samples from infected mice revealed a dramatic increase of IFN-γ in infected B6 IL-$10^{-/-}$ mice, relative to modest induction in B6 mice, confirming a systemic dysregulated inflammatory response in *B. burgdorferi* infected B6 IL-$10^{-/-}$ mice, (Fig 4A). Localized and systemic production of IFN-γ was thus hypothesized to be responsible for the increased arthritis severity in B6 IL-$10^{-/-}$ mice infected with *B. burgdorferi*. To directly assess involvement of IFN-γ, *B. burgdorferi* infected B6 IL-$10^{-/-}$ mice were treated with an IFN-γ-neutralizing antibody, an isotype control antibody, or PBS

alone, at 5-day intervals throughout the four-week *B. burgdorferi* infection. Arthritis severity at 4 weeks post infection in B6 IL-10$^{-/-}$ mice receiving PBS or control antibody injections was similar, and more severe than B6 control mice (Figure 4B). However, neutralization of IFN-γ in infected B6 IL-10$^{-/-}$ mice significantly reduced ankle swelling (Figure 4B) and histopathology scores (Table II). Interestingly, treatment of infected B6 IL-10$^{-/-}$ mice with the IFN-γ-neutralizing antibody had a modest effect on spirochete numbers in joint tissue relative to control B6 IL-10$^{-/-}$ mice (Figure 4C). Thus, the enhanced control of bacterial number in B6 IL-10$^{-/-}$ mice appears to be partially dependent on IFN-γ. We hypothesize that the other functions of IL-10, independent of suppressive effects on IFN-γ, may assist in host defense, as demonstrated by significant effect on mononuclear cell infiltration (addressed in the following sections and Table II). Taken together, these data suggest that IL-10 acts to suppress both arthritis and host defense via its regulatory effects on IFN-γ.

IFN-γ is required for early induction of interferon-responsive transcripts and for chemokines known to perpetuate recruitment of inflammatory cells

The ability of IFN-γ neutralization to suppress the severity of Lyme arthritis in B6 IL-10$^{-/-}$ mice, (Fig 4B, Table II), suggested it functioned locally through the induction of inflammatory response and chemokine production in the joint tissue. To characterize the involvement of IFN-γ early in the development of arthritis, prior to the end stage of disease, we assessed the presence of interferon-inducible transcripts at 2 weeks of infection in B6 IL-10$^{-/-}$ mice treated with PBS, isotype control antibody, or IFN-γ-neutralizing antibody. Consistent with previous results, interferon-inducible transcripts, including those for the chemokines *CXCL9* and *CXCL10*, were expressed at low levels in infected B6 mice and were highly upregulated in the joint tissue of infected B6 IL-10$^{-/-}$ mice injected with either PBS or control antibody (Figure 5A–D). In contrast, B6 IL-10$^{-/-}$ mice treated with IFN-γ-neutralizing antibody displayed a dramatic reduction in expression of these transcripts, similar to that seen in B6 mice (Figure 5A–D). These results, coupled with those of Figure 4B and Table II, implicate IFN-γ in both the up regulation of pro-inflammatory transcripts in the joint tissue beginning at 2 weeks of infection and in the increased severity of arthritis seen at 4 weeks of *B. burgdorferi* infection of B6 IL-10$^{-/-}$ mice.

Immune cell infiltration is regulated by IL-10 in infected B6 mice, and is partially dependent on IFN-γ

Histopathology of joint tissue from infected B6 IL-10$^{-/-}$ mice highlighted an IFN-γ-dependent increase in the mononuclear cell infiltrate (Table II). We reasoned that perhaps an early cellular infiltrate into the *B. burgdorferi*-infected joint tissue of B6 IL-10$^{-/-}$ mice should contain potential cellular sources of IFN-γ as well as interferon responsive transcripts. To characterize this cellular infiltrate into the infected joint, single cell suspensions were prepared from joint tissue from B6 and B6 IL-10$^{-/-}$ mice at 2 weeks post infection. Increased frequencies of T cells, NK cells, NKT cells, and macrophages were observed into the joint tissue of both B6 and B6 IL-10$^{-/-}$ mice, relative to uninfected controls (Figure 6A–B) at 2 weeks of infection. Levels of T cells, NK T cells, and macrophages were 2–3 fold greater in joint tissue of infected B6 IL-10$^{-/-}$ mice than in B6 mice (Figure 6A, iv and 6B, iv). Many of these cell types have been reported to produce IFN-γ during *B. burgdorferi* infection, as well as in other infection models. Because neutralization of IFN-γ in B6 IL-10$^{-/-}$ mice resulted in a decreased mononuclear infiltrate into the joint tissue of B6 IL-10$^{-/-}$ mice (Table II), and this cytokine was also required for the expression of chemokines (*CXCL9* and *CXCL10*) known to play a role in the recruitment of NK cells, T cells, and macrophages, it was hypothesized that IFN-γ would be required for the infiltration of one or more of these cells types. To test this hypothesis, B6 IL-10$^{-/-}$ mice were treated with the IFN-γ-neutralizing antibody during a 2-week *B. burgdorferi* infection.

Low levels of infiltrating T cells, NK cells, NKT cells, and macrophages were observed in the infected joint tissue of B6 mice at 2 weeks of infection, but high levels of these cells were observed in the infected joint tissue of B6 IL-$10^{-/-}$ mice at the same interval (Figure 6C–F). In contrast, B6 IL-$10^{-/-}$ mice treated with the IFN-γ-neutralizing antibody had significantly fewer numbers of infiltrating NK and NKT cells (Figure 6C–D), indicating strong dependence on localized effects of IFN-γ. The finding that the number of infiltrating macrophages and T cells in the joint were not reduced by IFN-γ neutralization suggests that recruitment of these cells is not solely dependent on IFN-γ (Fig 6E–F), but that their infiltration is regulated by IL-10. This may explain the modest effect of IFN-γ neutralization on enhanced bacterial control in the joint tissue of B6 IL-$10^{-/-}$ mice, which was less dependent on IFN-γ than was arthritis development (Figure 4B).

Multiple cell types recruited to the infected joint tissue of B6 IL-$10^{-/-}$ mice produce IFN-γ

Canonical sources of IFN-γ include T_H1 polarized CD4 T cells, NK cells and NKT cells, all of which are found in the joint tissue of *B. burgdorferi* infected B6 IL-$10^{-/-}$ mice and have been previously associated with IFN-γ production during *B. burgdorferi* infection (17, 21, 42, 45–48). Although B cells from the infected lymph node have also been linked to IFN-γ production (49), $B220^+$ cells were not detected in the infected joint tissue of B6 or B6 IL-$10^{-/-}$ mice (Figure 2D iv, and data not shown). To identify the cell types responsible for IFN-γ production, as well as interferon-inducible gene expression in the joint tissue, B6 IL-$10^{-/-}$ mice were injected with GK1.5, a CD4 T cell-depleting antibody, or PK136, an NK/NKT cell-depleting antibody, followed by periodic booster injections of depleting antibody during the course of infection with *B. burgdorferi*. Only depletion of $CD4^+$ T cells reduced the presence of IFN-γ in the serum of infected B6 IL-$10^{-/-}$ mice, suggesting these cells are the most important source driving systemic production of IFN-γ (Figure 7A). Depletion of $CD4^+$ T cells, but not NK cells, resulted in a significant reduction in *CXCL9* transcripts, but only a modest reduction of *CXCL10* transcripts in the joint tissue at 2 weeks of infection in B6 IL-$10^{-/-}$ mice, (Fig 7B–C). This suggests either that depletion of suspected cell types was insufficient in the joint, or that multiple cell types produce IFN-γ in response to *B. burgdorferi* spirochetes in the joint.

To identify the joint infiltrating cells responsible for the production of IFN-γ, single cell suspensions of joint tissue were prepared from B6 IL-$10^{-/-}$ mice two weeks post infection, labeled for lineage markers, and FACS was utilized to sort specific populations. Total RNA was then extracted from the sorted cells, and IFN-γ, and lineage specific markers were quantified by RT-PCR in each fraction. Cell lineages were defined in the following manner: NK cells as $NK1.1^+$ TCR-β^-; NKT cells as $NK1.1^+$, TCR-β^+; $CD4^+$ T cells as $NK1.1^-$, TCR-β^+, and $CD4^+$, and Macrophages $F4/80^+$. IFN-γ transcripts were highly enriched in sorted fractions containing NK cells and $CD4^+$ T cells recovered from the infected joint tissue of B6 IL-$10^{-/-}$ mice, but no enrichment of IFN-γ was observed in sorted NKT cells, macrophages, un-fractionated joint cells (Figure 8A), or whole joint (Figure 1B). Thus, as was previously postulated (Figure 7), two cell types, NK cells and CD^+ T cells, but not NKT cells, are responsible for localized production of IFN-γ in *B. burgdorferi* infected B6 IL-$10^{-/-}$ mice.

To confirm that the failure to detect IFN-γ transcripts in the NKT cell or other fractions did not reflect a poor recovery of cells, lineage specific transcripts from each of the fractions were assessed by RT-PCR. CD49b (α2 integrin expressed by NK and NKT cells) transcripts were enriched in both the NK cell and NKT cell fractions (Figure 8B) as expected, while expression of the NKT cell specific, Vα14-Jα18 iTCR, was found to be enriched only in the sorted NKT cell fraction (Figure 8C). CD4 transcripts were enriched in the CD4 T cell fraction (Figure 8D). Because others have reported that NKT cells in some locations fail to express NK1.1 an additional experiment was performed in which NKT cells in the joint

were analyzed using CD1d tetramers to allow identification of the dominant population of NKT cells (50). Tetramer positive cells were extremely rare (0.1% of total joint cells), but 86% were positive for both NK1.1 and TCR-β, suggesting our characterization of this population was inclusive.

Discussion

The IL-10$^{-/-}$ mouse has proven to be a useful tool in the study of the inflammatory response to *B. burgdorferi* on both the arthritis resistant B6 and arthritis susceptible C3H backgrounds (36, 43). An important feature of this model is that the heightened inflammatory response permitted in the absence of IL-10 results in 5–10 fold fewer spirochetes in the joint tissue (36, 43), unlike many other immunodeficiencies, which result in higher levels of tissue spirochetes. Thus, a unique feature of this model is the observation that very low levels of antigen are capable of triggering an exuberant inflammatory response. Increased arthritis severity in these mice is hypothesized to be due to the collateral damage caused by a poorly regulated immune response. In the human Lyme disease patient population there are rare individuals who continue to display signs of infection even following a regimen of therapy expected to eradicate the spirochetes (5, 9). In some reports, these individuals are treated with anti-inflammatory drugs used for rheumatoid arthritis (51), after which most signs of infection resolve. Hence, we hypothesize that the B6 IL-10$^{-/-}$ mouse may provide insight into the involvement of dysregulated response to the initial triggering effect of tissue infiltrating *B. burgdorferi*, and that this may result in delayed resolution of arthritis.

Previous gene expression analysis of joint tissue from *B. burgdorferi* -infected mice revealed an interferon-inducible response that correlated to increased arthritis severity in C3H and B6 IL-10$^{-/-}$ mice (39). While this response was early (1 week of infection), and evanescent in C3H mice, it was delayed (2 weeks) and sustained (4 weeks) in B6 IL-10$^{-/-}$ mice. Importantly, only the B6 IL-10$^{-/-}$ mouse displayed induced expression of any interferon gene, with IFN-γ transcripts increased by 16-and 22-fold at 2 and 4 weeks of infection, respectively (39). A final critical difference between C3H and B6 IL-10$^{-/-}$ mice was that the most robustly upregulated transcripts in C3H mice were for a group of GTPases, whereas in B6 IL-10$^{-/-}$ mice, the chemokines *CXCL9* and *CXCL10* were most prominent. In the present study, systemic production of IFN-γ was also observed in B6 IL-10$^{-/-}$ mice (Figure 4A), which suggested arthritis developed in these mice could be due to failed regulation of IFN-γ expression in the infected joint tissue. Indeed, neutralization of IFN-γ reduced arthritis severity (Figure 4A, Table 1), suppressed the expression of the interferon-inducible transcripts *CXCL9* and *CXCL10* (Figure 5A,B), and limited the early infiltration of NK and NKT cells into the infected joints of B6 IL-10$^{-/-}$ mice (Figure 6C,D; Figure 9B,C,E). Joint histopathology also demonstrated a reduced mononuclear infiltrate in B6 IL-10$^{-/-}$ mice treated with anti-IFN-γ. The observation that infected B6 IL-10$^{-/-}$ mice harbor more macrophages in their joint tissue than B6 mice (Figure 6B,F) provides a possible explanation for the enhanced host defense observed in B6 IL-10$^{-/-}$ mice, and supports the conclusion made by Lazarus *et al*, that innate immunity is responsible for the enhanced host defense seen in B6 IL-10$^{-/-}$ mice (52). This enhanced host defense phenotype was partially abrogated in mice receiving anti-IFN-γ (Figure 4C). While the upstream events that culminate in sustained production of IFN-γ were not identified, mediation by IL-12 is a possibility as *B. burgdorferi* stimulated B6 IL-10$^{-/-}$ macrophages produced 5 to 10 fold more of this cytokine than B6 macrophages (unpublished observation).

These findings highlight a critical difference in arthritis development between C3H and B6 IL-10$^{-/-}$ mice. Whereas arthritis development in C3H mice is dependant on Type I interferon and occurs in the absence of IFN-γ (16, 21), our results demonstrate that IFN-γ is required for arthritis development in B6 IL-10$^{-/-}$ mice. Thus we conclude that both Type I

and Type II interferon pathways can influence arthritis development, given the correct circumstances. Although many of the downstream effectors are identical between Type I and Type II interferon signaling, the mechanisms for arthritis development between C3H and B6 IL-$10^{-/-}$ mice appears to be distinct. Of interest was the previous finding that the addition of exogenous IL-10 via adenoviral delivery failed to suppress arthritis development in C3H mice (43). This may reflect failure of IL-10 to regulate the Type I IFN pathway inherent in the C3H mouse, and further suggests that Type I IFN masks pro-arthritic contributions of IFNγ in infected C3H mice (16, 21, 39). This supports the observation that Lyme arthritis can occur via multiple mechanisms as assessed by genetic linkage analysis, where several pathways have been implicated in Lyme arthritis development (53, 54).

B. burgdorferi induction of IFN-γ has been observed both *in vitro* and *in vivo* for multiple mouse strains and cell types, as well as in human PBMC's (55–57). In C3H mice, depletion of NK and NKT cells resulted in reduced expression of most interferon-inducible genes, in a near identical fashion to IFN-γ neutralization in C3H mice (21). Other studies have linked NKT cells to IFN-γ in murine Lyme carditis but the link to arthritis was only seen on the BALB/c background (42, 47). In a study using high dose inoculum of *B. burgdorferi* administered intravenously, mice deficient in NKT cells were found to harbor high levels of spirochetes in joint tissue at 3 days, suggesting they could provide an early source of systemic anti-microbial IFN-γ (48). In carditis, IFN-γ signaling limits pathology and serves to activate local macrophages and induce killing of *B. burgdorferi* spirochetes (42). Our finding indicate that $CD4^+$ T cells, but not NK/NKT cells, are responsible for the high levels of IFN-γ in the serum of infected B6 IL-$10^{-/-}$ mice (Figure 7A), whereas both $CD4^+$ T cells and NK cells are the major sources of IFN-γ in the joint tissue of infected B6 IL-$10^{-/-}$ mice (Figure 8A; Figure 9).

The critical role of IL-10 in suppressing tissue specific induction of interferon-inducible genes and Lyme arthritis development in B6 mice suggested that early and consistent local production of IL-10 would be necessary to suppress arthritis severity. A variety of cell types are capable of producing IL-10, including components of both the innate and adaptive immune response and other cell types associated with tissue function and vasculature including synoviocytes (58, 59). In this study, two approaches were employed to link IL-10 to its cellular source in the infected joint. Both radiation chimeras and the IL-10 reporter mouse demonstrated that leukocytes were the primary sources of IL-10 expression in the infected joint, although other cell types such as fibroblast-like synoviocytes were not specifically addressed and could be additional sources of the cytokine (59). Furthermore, both $CD4^+$ T cells and $F4/80^+$ macrophages were found to express IL-10 in infected joint tissue with comparable contributions of the detectable GFP reporter (Figure 2D–F; Table I; Figure 9). Although the subset of $CD4^+$T cell responsible for IL-10 production was not indentified in this study, we suspect involvement of T_H2, T_{reg}, or even the newly identified T_r1 subset of $CD4^+$ T cells. The finding that $FoxP3^+$ T_{reg} cells in the joint were significantly fewer than the total IL-10-producing $CD4^+$ T cells suggested that the $CD4^+$ T cell subset(s) responsible for *IL-10* expression consist of many non-T_{reg} cells. The peak of *IL-10* expression in the joint occurs at 11 days post infection, and prior to the development of arthritis. This suggests that IL-10 has a dampening effect on localized inflammation, and serves to limit disease severity, rather than resolve it. The early suppressive effects of IL-10 are robust and pleiotropic, as they limit expression of interferon-inducible genes, pro-inflammatory cytokines, and cellular infiltrates into the joint through regulation of IFN-γ-dependant and IFN-γ-independent pathways. The primary function of IL-10 in arthritis development is to suppress expression of IFN-γ, which is required for arthritis development in B6 IL-$10^{-/-}$ mice.

The B6 IL-10$^{-/-}$ mouse model provides a much-needed model for studying the role of IFN-γ in Lyme arthritis development. While complete IL-10 deficiency represents an extreme example of dysregulated inflammation, a host of factors could influence a prolonged inflammatory response. An important finding of the current study is demonstration that CD4^{+} T cells in the infected joint can produce both pro and anti-arthritic cytokines, and that loss of the anti-inflammatory signal results in increased disease severity. This observation suggests a dominant effect of anti-inflammatory signaling, and that any number of events could combine to disrupt a delicate balance between bactericidal and pathologic inflammation. Interestingly, a loss of function polymorphism in the human *il10r1* gene has recently been reported (60–63), and is associated with risk for extra-pulmonary tuberculosis and rheumatoid arthritis (60, 63). While it is unlikely that treatment-refractory Lyme arthritis patients test positive for these polymorphisms, the end results among these patients and B6 IL-10$^{-/-}$ mice are similar, in the elevated expression of IFN-γ and IFN-γ-inducible chemokines, and possibly represent the result of an insufficient regulatory response.

Acknowledgments

We thank Kenneth C. Bramwell, Robert Lochhead, Jennifer C. Miller and members of the John Weis Lab, for helpful discussion during the course of this study. We thank Matt Williams and his lab for their tutelage in the art of flow cytometry. We also thank Tom Greene and Jian Ying of the University of Utah Biostatistics Center for their guidance.

References

1. Steere AC, Coburn J, Glickstein L. The emergence of Lyme disease. The Journal of clinical investigation. 2004; 113:1093–1101. [PubMed: 15085185]
2. Burgdorfer W, Barbour AG, Hayes SF, Benach JL, Grunwaldt E, Davis JP. Lyme disease: a tick-borne spirochetosis? Science (New York, N.Y. 1982; 216:1317–1319.
3. Hayes EB, Piesman J. How can we prevent Lyme disease? N Engl J Med. 2003; 348:2424–2430. [PubMed: 12802029]
4. Steere AC, Grodzicki RL, Kornblatt AN, Craft JE, Barbour AG, Burgdorfer W, Schmid GP, Johnson E, Malawista SE. The spirochetal etiology of Lyme disease. N Engl J Med. 1983; 308:733–740. [PubMed: 6828118]
5. Steere AC, Glickstein L. Elucidation of Lyme arthritis. Nature reviews. 2004; 4:143–152.
6. Steere AC, Schoen RT, Taylor E. The clinical evolution of Lyme arthritis. Ann Intern Med. 1987; 107:725–731. [PubMed: 3662285]
7. Wormser GP, Dattwyler RJ, Shapiro ED, Halperin JJ, Steere AC, Klempner MS, Krause PJ, Bakken JS, Strle F, Stanek G, Bockenstedt L, Fish D, Dumler JS, Nadelman RB. The clinical assessment, treatment, and prevention of lyme disease, human granulocytic anaplasmosis, and babesiosis: clinical practice guidelines by the Infectious Diseases Society of America. Clin Infect Dis. 2006; 43:1089–1134. [PubMed: 17029130]
8. Schoen RT. A case revealing the natural history of untreated Lyme disease. Nat Rev Rheumatol. 2011; 7:179–184. [PubMed: 21173795]
9. Shin JJ, Glickstein LJ, Steere AC. High levels of inflammatory chemokines and cytokines in joint fluid and synovial tissue throughout the course of antibiotic-refractory lyme arthritis. Arthritis Rheum. 2007; 56:1325–1335. [PubMed: 17393419]
10. Barthold SW, Persing DH, Armstrong AL, Peeples RA. Kinetics of *Borrelia burgdorferi* dissemination and evolution of disease after intradermal inoculation of mice. American Journal of Pathology. 1991; 139:263–273. [PubMed: 1867318]
11. Ma Y, Seiler KP, Eichwald EJ, Weis JH, Teuscher C, Weis JJ. Distinct characteristics of resistance to *Borrelia burgdorferi*-induced arthritis in C57BL/6N mice. Infection & Immunity. 1998; 66:161–168. [PubMed: 9423853]

12. Morrison TB, Ma Y, Weis JH, Weis JJ. Rapid and sensitive quantification of Borrelia burgdorferi-infected mouse tissues by continuous fluorescent monitoring of PCR. J Clin Microbiol. 1999; 37:987–992. [PubMed: 10074514]
13. Barthold SW, Beck DS, Hansen GM, Terwilliger GA, Moody KD. Lyme borreliosis in selected strains and ages of laboratory mice. Journal of Infectious Diseases. 1990; 162:133–138. [PubMed: 2141344]
14. Brown CR, Reiner SL. Clearance of Borrelia burgdorferi may not be required for resistance to experimental lyme arthritis. Infect Immun. 1998; 66:2065–2071. [PubMed: 9573090]
15. Matyniak JE, Reiner SL. T helper phenotype and genetic susceptibility in experimental Lyme disease. Journal of Experimental Medicine. 1995; 181:1251–1254. [PubMed: 7869043]
16. Brown CR, Reiner SL. Experimental lyme arthritis in the absence of interleukin-4 or gamma interferon. Infect Immun. 1999; 67:3329–3333. [PubMed: 10377109]
17. Glickstein L, Edelstein M, Dong JZ. Gamma interferon is not required for arthritis resistance in the murine Lyme disease model. Infect Immun. 2001; 69:3737–3743. [PubMed: 11349038]
18. Keane-Myers A, Nickell SP. Role of IL-4 and IFN-g in modulation of immunity to *Borrelia burgdorferi* in mice. J. Immunol. 1995; 155:2020–2028. [PubMed: 7636253]
19. Potter MR, Noben-Trauth N, Weis JH, Teuscher C, Weis JJ. Interleukin-4 (IL-4) and IL-13 signaling pathways do not regulate *Borrelia burgdorferi*-induced arthritis in mice: IgG1 is not required for host control of tissue spirochetes. Infect Immun. 2000; 68:5603–5609. [PubMed: 10992460]
20. Barthold SW, Sidman CL, Smith AL. Lyme borreliosis in genetically resistant and susceptible mice with severe combined immunodeficiency. Am J Trop Med Hyg. 1992; 47:605–613. [PubMed: 1449201]
21. Miller JC, Ma Y, Bian J, Sheehan KC, Zachary JF, Weis JH, Schreiber RD, Weis JJ. A critical role for type I IFN in arthritis development following Borrelia burgdorferi infection of mice. J Immunol. 2008; 181:8492–8503. [PubMed: 19050267]
22. Heilpern AJ, Wertheim W, He J, Perides G, Bronson RT, Hu LT. Matrix metalloproteinase 9 plays a key role in lyme arthritis but not in dissemination of Borrelia burgdorferi. Infect Immun. 2009; 77:2643–2649. [PubMed: 19364840]
23. Brown CR, Blaho VA, Loiacono CM. Susceptibility to experimental Lyme arthritis correlates with KC and monocyte chemoattractant protein-1 production in joints and requires neutrophil recruitment via CXCR2. J Immunol. 2003; 171:893–901. [PubMed: 12847259]
24. Benhnia MR, Wroblewski D, Akhtar MN, Patel RA, Lavezzi W, Gangloff SC, Goyert SM, Caimano MJ, Radolf JD, Sellati TJ. Signaling through CD14 attenuates the inflammatory response to Borrelia burgdorferi, the agent of Lyme disease. J Immunol. 2005; 174:1539–1548. [PubMed: 15661914]
25. Duray PH. Histopathology of clinical phases of human Lyme disease. Rheum Dis Clin North Am. 1989; 15:691–710. [PubMed: 2685926]
26. Gross DM, Steere AC, Huber BT. T helper 1 response is dominant and localized to the synovial fluid in patients with Lyme arthritis. J Immunol. 1998; 160:1022–1028. [PubMed: 9551943]
27. Roessner K, Wolfe J, Shi C, Sigal LH, Huber S, Budd RC. High expression of Fas ligand by synovial fluid-derived gamma delta T cells in Lyme arthritis. J Immunol. 2003; 170:2702–2710. [PubMed: 12594300]
28. Vincent MS, Roessner K, Lynch D, Wilson D, Cooper SM, Tschopp J, Sigal LH, Budd RC. Apoptosis of Fashigh CD4+ synovial T cells by borrelia-reactive Fas-ligand(high) gamma delta T cells in Lyme arthritis. The Journal of experimental medicine. 1996; 184:2109–2117. [PubMed: 8976167]
29. Barthold SW, de Souza M. Exacerbation of Lyme Arthritis in beige mice. J Inf Dis. 1995; 172:778–784. [PubMed: 7658072]
30. Wang X, Ma Y, Yoder A, Crandall H, Zachary JF, Fujinami RS, Weis JH, Weis JJ. T cell infiltration is asoociated with increased Lyme arthritis in TLR2−/− mice. FEMS Immunol. Med. Microbiol. 2008; 52:124–133. [PubMed: 18081848]

31. Bolz DD, Sundsbak RS, Ma Y, Akira S, Kirschning CJ, Zachary JF, Weis JH, Weis JJ. MyD88 plays a unique role in host defense but not arthritis development in Lyme disease. J Immunol. 2004; 173:2003–2010. [PubMed: 15265935]
32. Anguita J, Barthold SW, Persinski R, Hedrick MN, Huy CA, Davis RJ, Flavell RA, Fikrig E. Murine Lyme arthritis development mediated by p38 mitogen-activated protein kinase activity. J Immunol. 2002; 168:6352–6357. [PubMed: 12055252]
33. Anguita J, Rincon M, Samanta S, Barthold SW, Flavell RA, Fikrig E. Borrelia burgdorferi-infected, interleukin-6-deficient mice have decreased Th2 responses and increased lyme arthritis. J Infect Dis. 1998; 178:1512–1515. [PubMed: 9780277]
34. Wooten RM, Ma Y, Yoder RA, Brown JP, Weis JH, Zachary JF, Kirschning CJ, Weis JJ. Toll-like receptor 2 is required for innate, but not acquired, host defense to Borrelia burgdorferi. Journal of immunology. 2002; 168(1):348–355.
35. Iliopoulou BP, Alroy J, Huber BT. CD28 deficiency exacerbates joint inflammation upon Borrelia burgdorferi infection, resulting in the development of chronic Lyme arthritis. J Immunol. 2007; 179:8076–8082. [PubMed: 18056348]
36. Brown JP, Zachary JF, Teuscher C, Weis JJ, Wooten RM. Dual Role of Interleukin-10 in Murine Lyme Disease: Regulation of Arthritis Severity and Host Defense. Infect Immun. 1999; 67:5142–5150. [PubMed: 10496888]
37. Londono D, Marques A, Hornung RL, Cadavid D. Relapsing fever borreliosis in interleukin-10-deficient mice. Infect Immun. 2008; 76:5508–5513. [PubMed: 18794280]
38. Dennis VA, Jefferson A, Singh SR, Ganapamo F, Philipp MT. Interleukin-10 anti-inflammatory response to Borrelia burgdorferi, the agent of Lyme disease: a possible role for suppressors of cytokine signaling 1 and 3. Infect Immun. 2006; 74:5780–5789. [PubMed: 16988256]
39. Crandall H, Dunn DM, Ma Y, Wooten RM, Zachary JF, Weis JH, Weiss RB, Weis JJ. Gene expression profiling reveals unique pathways associated with differential severity of Lyme arthritis. J. Immunol. 2006; 177:7930–7942. [PubMed: 17114465]
40. Huang X, Pierce LJ, Cobine PA, Winge DR, Spangrude GJ. Copper modulates the differentiation of mouse hematopoietic progenitor cells in culture. Cell Transplant. 2009; 18:887–897. [PubMed: 19520051]
41. Chirgwin JM, Przybyla AE, MacDonald RJ, Rutter WJ. Isolation of biologically active ribonucleic acid from sources enriched in ribonuclease. Biochemistry. 1979; 18:5294–5299. [PubMed: 518835]
42. Olson CM Jr, Bates TC, Izadi H, Radolf JD, Huber SA, Boyson JE, Anguita J. Local production of IFN-gamma by invariant NKT cells modulates acute Lyme carditis. J Immunol. 2009; 182:3728–3734. [PubMed: 19265151]
43. Brown CR, Lai AY, Callen ST, Blaho VA, Hughes JM, Mitchell WJ. Adenoviral delivery of interleukin-10 fails to attenuate experimental Lyme disease. Infect Immun. 2008; 76:5500–5507. [PubMed: 18824530]
44. Kamanaka M, Kim ST, Wan YY, Sutterwala FS, Lara-Tejero M, Galan JE, Harhaj E, Flavell RA. Expression of interleukin-10 in intestinal lymphocytes detected by an interleukin-10 reporter knockin tiger mouse. Immunity. 2006; 25:941–952. [PubMed: 17137799]
45. Ma Y, Seiler KP, Tai K, Yang L, Woods M, Weis JJ. Outer surface lipoproteins of Borrelia burgdorferi stimulate nitric oxide production by the cytokine-inducible pathway. Infect Immun. 1994; 62:3663–3671. [PubMed: 7520417]
46. Bockenstedt L, Kang KI, Chang C, Persing D, Hayday A, Barthold SW. CD4+ T helper 1 cells facilitate regression of murine Lyme carditis. Infect Immun. 2001; 69:5264–5269. [PubMed: 11500394]
47. Tupin E, Benhnia MR, Kinjo Y, Patsey R, Lena CJ, Haller MC, Caimano MJ, Imamura M, Wong CH, Crotty S, Radolf JD, Sellati TJ, Kronenberg M. NKT cells prevent chronic joint inflammation after infection with Borrelia burgdorferi. Proc Natl Acad Sci U S A. 2008; 105:19863–19868. [PubMed: 19060201]
48. Lee WY, Moriarty TJ, Wong CH, Zhou H, Strieter RM, van Rooijen N, Chaconas G, Kubes P. An intravascular immune response to Borrelia burgdorferi involves Kupffer cells and iNKT cells. Nature immunology. 2010; 11:295–302. [PubMed: 20228796]

49. Ganapamo F, Dennis VA, Philipp MT. CD19(+) cells produce IFN-gamma in mice infected with Borrelia burgdorferi. European journal of immunology. 2001; 31:3460–3468. [PubMed: 11745365]
50. Doisne JM, Becourt C, Amniai L, Duarte N, Le Luduec JB, Eberl G, Benlagha K. Skin and peripheral lymph node invariant NKT cells are mainly retinoic acid receptor-related orphan receptor (gamma)t+ and respond preferentially under inflammatory conditions. J Immunol. 2009; 183:2142–2149. [PubMed: 19587013]
51. Steere AC, Angelis SM. Therapy for Lyme arthritis: strategies for the treatment of antibiotic-refractory arthritis. Arthritis Rheum. 2006; 54:3079–3086. [PubMed: 17009226]
52. Lazarus JJ, Meadows MJ, Lintner RE, Wooten RM. IL-10 deficiency promotes increased Borrelia burgdorferi clearance predominantly through enhanced innate immune responses. J Immunol. 2006; 177:7076–7085. [PubMed: 17082624]
53. Weis JJ, McCracken BA, Ma Y, Fairbairn D, Roper RJ, Morrison TB, Weis JH, Zachary JF, Doerge RW, Teuscher C. Identification of quantitative trait loci governing arthritis severity and humoral responses in the murine model of Lyme disease. J Immunol. 1999; 162:948–956. [PubMed: 9916719]
54. Roper RJ, Weis JJ, McCracken BA, Green CB, Ma Y, Weber KS, Fairbairn D, Butterfield RJ, Potter MR, Zachary JF, Doerge RW, Teuscher C. Genetic control of susceptibility to experimental Lyme arthritis is polygenic and exhibits consistent linkage to multiple loci on chromosome 5 in four independent mouse crosses. Genes Immun. 2001; 2:388–397. [PubMed: 11704805]
55. Petzke MM, Brooks A, Krupna MA, Mordue D, Schwartz I. Recognition of Borrelia burgdorferi, the Lyme disease spirochete, by TLR7 and TLR9 induces a type I IFN response by human immune cells. J Immunol. 2009; 183:5279–5292. [PubMed: 19794067]
56. Moore MW, Cruz AR, LaVake CJ, Marzo AL, Eggers CH, Salazar JC, Radolf JD. Phagocytosis of Borrelia burgdorferi and Treponema pallidum potentiates innate immune activation and induces gamma interferon production. Infect Immun. 2007; 75:2046–2062. [PubMed: 17220323]
57. Salazar JC, Duhnam-Ems S, La Vake C, Cruz AR, Moore MW, Caimano MJ, Velez-Climent L, Shupe J, Krueger W, Radolf JD. Activation of human monocytes by live Borrelia burgdorferi generates TLR2-dependent and -independent responses which include induction of IFNB. PLoS Pathog. 2009; 5:e1000444. [PubMed: 19461888]
58. Couper KN, Blount DG, Riley EM. IL-10: the master regulator of immunity to infection. J Immunol. 2008; 180:5771–5777. [PubMed: 18424693]
59. Ritchlin C, Haas-Smith SA. Expression of interleukin 10 mRNA and protein by synovial fibroblastoid cells. J Rheumatol. 2001; 28:698–705. [PubMed: 11327238]
60. Ben-Selma W, Harizi H, Boukadida J. Association of TNF-alpha and IL-10 polymorphisms with tuberculosis in Tunisian populations. Microbes Infect. 2011
61. Zhang J, Chen Y, Nie XB, Wu WH, Zhang H, Zhang M, He XM, Lu JX. Interleukin-10 polymorphisms and tuberculosis susceptibility: a meta-analysis. Int J Tuberc Lung Dis. 2011; 15:594–601. [PubMed: 21756510]
62. Zhang X, Wang Z, Fan J, Liu G, Peng Z. Impact of interleukin-10 gene polymorphisms on tacrolimus dosing requirements in Chinese liver transplant patients during the early posttransplantation period. Eur J Clin Pharmacol. 2011; 67:803–813. [PubMed: 21359536]
63. Hermann J, Gruber S, Neufeld JB, Grundtner P, Graninger M, Graninger WB, Berghold A, Gasche C. IL10R1 loss-of-function alleles in rheumatoid arthritis and systemic lupus erythematosus. Clin Exp Rheumatol. 2009; 27:603–608. [PubMed: 19772791]

Abbreviations

7'AAD	7-aminoactinocycin D
MFI	mean fluorescence intensity
NKT cell	natural killer T cell

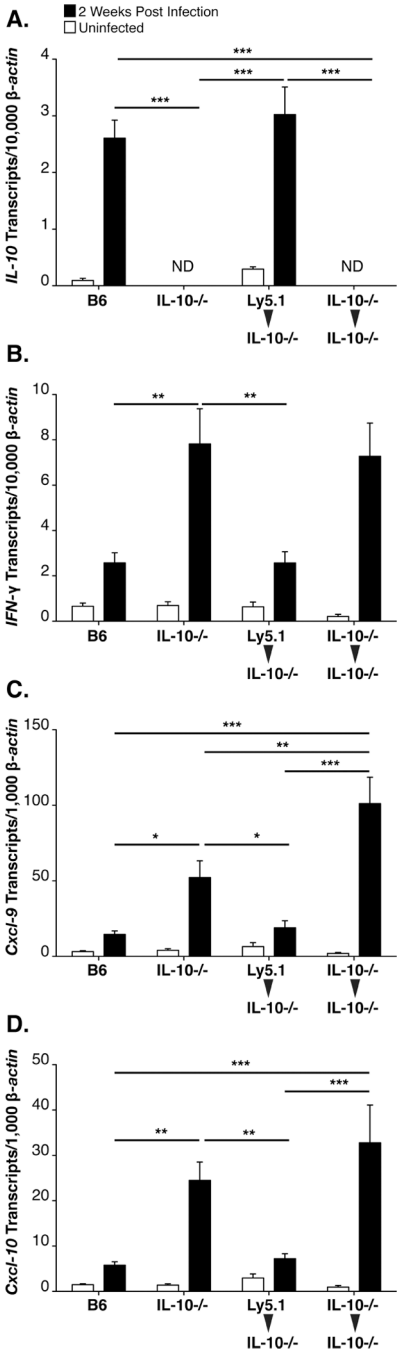

Figure 1. A hematopoietic source of IL-10 regulates expression of interferon-inducible transcripts

RT-PCR analysis of joint tissue at 2 weeks post infection with *B. burgdorferi* from B6 (N=8), B6 IL-10$^{-/-}$ (N=8), LY5.1→ B6 IL-10$^{-/-}$ chimeras (N=8), and B6 IL-10$^{-/-}$→ B6 IL-10$^{-/-}$ chimeras (N=6). Expression of *IL-10* (A), *IFN-γ* (B), *CXCL9* (C), and *CXCL10* (D), was normalized to *β-actin*. The term 'ND' indicates that *IL-10* transcripts were not detected (A). Statistical analysis was performed as described in Materials and Methods.

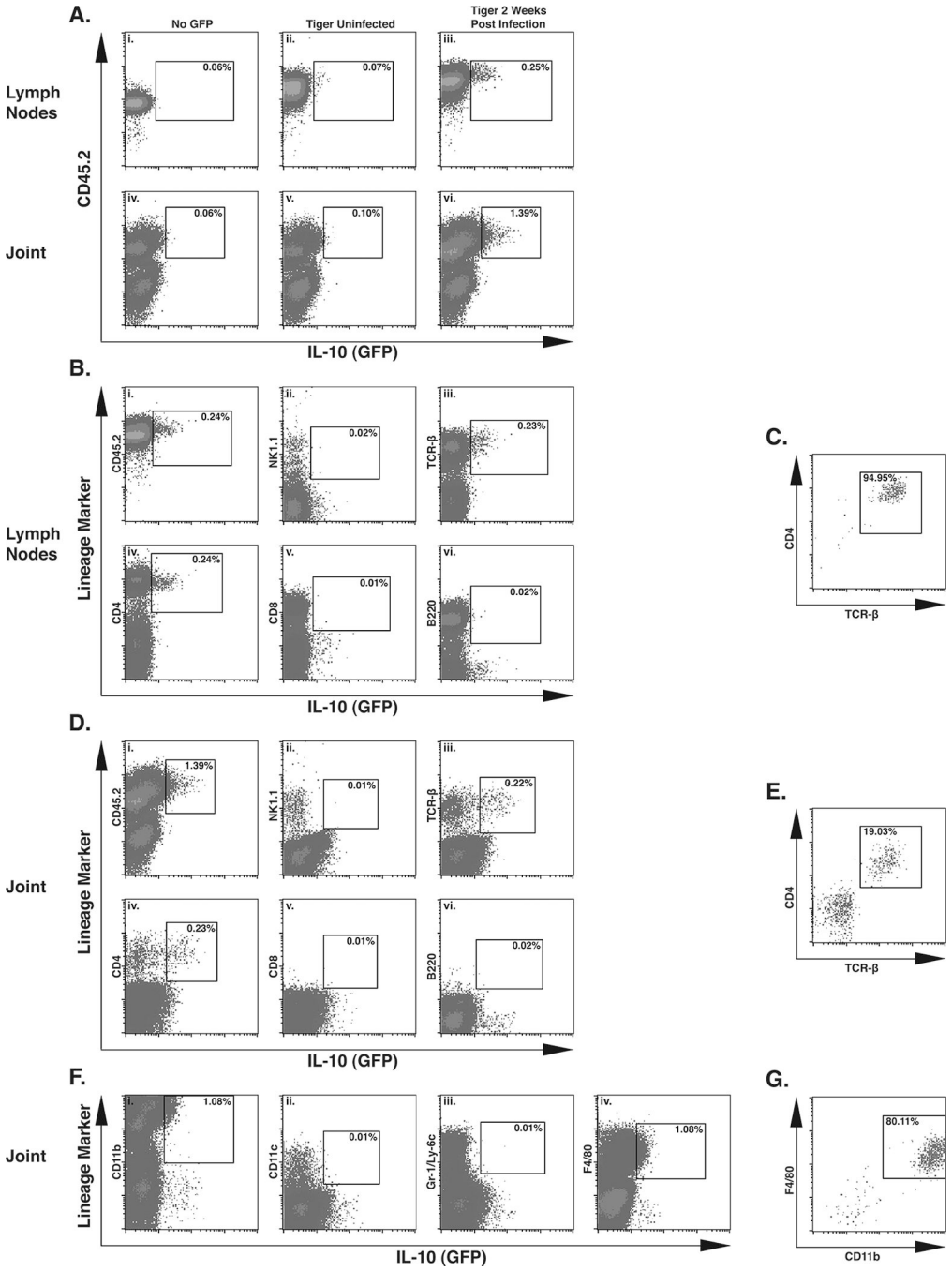

Figure 2. IL-10 expression in vivo is found in both CD4$^+$ T cells and macrophages

The IL-10 GFP reporter mouse strain designated '*tiger*' was used to identify cellular sources of IL-10 in the joint *in vivo*. Flow cytometry data in A–E utilized primarily lymphoid markers to designate populations, while date from F–G represent a separate myeloid analysis. Gate boundaries for GFP and lineage markers were established by isotype control staining in cells derived from non-*tiger* mice. Data from A-iii, vi, and B–G were acquired from a single infected *tiger* mouse at 2 weeks post infection. Analysis of 3 infected *tiger* mice yielded similar results. IL-10 (GFP) expression in CD45$^+$ cells from infected tiger mice, in both the lymph nodes (A-iii) and joint tissue (A-vi). IL-10 (GFP) expression in the tissues of non-tiger or uninfected tiger mice (Ai, ii, iv, v). Analysis of lineage-specific

surface markers that were present on IL-10 $(GFP)^+$ cells in infected lymph nodes (B). Frequency of $CD4^+$, TCR-β^+ T cells in the total IL-10 $(GFP)^+$ cells in lymph node tissue (C). Analysis of lymphocyte lineage-specific surface markers that were present on IL-10 $(GFP)^+$ cells in infected joint tissue (D). Frequency of $CD4^+$, TCR-β^+ T cells in the total IL-10 $(GFP)^+$ cells in infected joint tissue (E). Analysis of myeloid lineage-specific surface markers that were present on IL-10 $(GFP)^+$ cells in infected joint tissue (F). Frequency of $CD11b^+$, $F4/80^+$ macrophages in the total IL-10 $(GFP)^+$ cells in infected joint tissue (G).

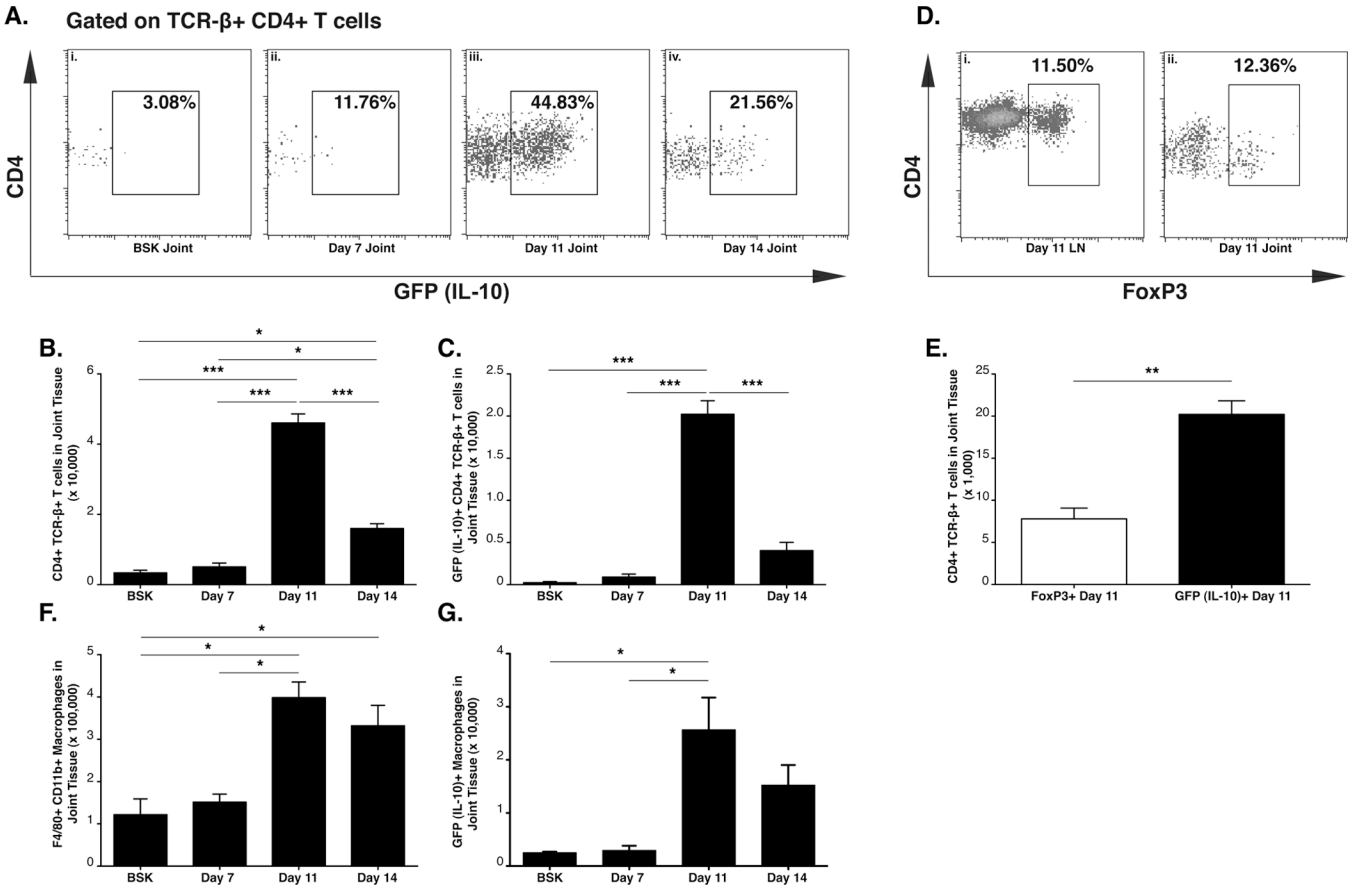

Figure 3. Kinetic analysis of IL-10 expressing cells in tiger mice

Control and infected IL-10 GFP reporter mouse '*tiger*' (N=3 per group) were analyzed for IL-10 (GFP) producing $CD4^+$ T cells and macrophages in joint tissue. Flow cytometry analysis of IL-10 expression in joint $CD4^+$ TCR-β^+ T cells from uninfected mice (A-i), or mice at day 7 post infection (A-ii), day 11 post infection (A-iii), and day 14 post infection (A-iv). Total joint $CD4^+$ TCR-β^+ T cells (B) and total IL-10 $(GFP)^+$ $CD4^+$ TCR-β^+ T cells (C). Frequency of $CD4^+$ TCR-β^+ $FoxP3^+$ T_{reg} cells in lymph nodes and joint tissue at day 11 post infection (D). Comparison of total joint IL-10 $(GFP)^+$ $CD4^+$ TCR-β^+ T cells and total joint $CD4^+$ TCR-β^+ $FoxP3^+$ T_{reg} cells in joint tissue at day 11 post infection (E). Total $CD11b^+$, $F4/80^+$ macrophages (F), and IL-10 $(GFP)^+$ $CD11b^+$, $F4/80^+$ macrophages (G) in joint tissue. Statistical analyses were performed as reported in Materials and Methods. Statistical significance in (E) was determined using student's T test.

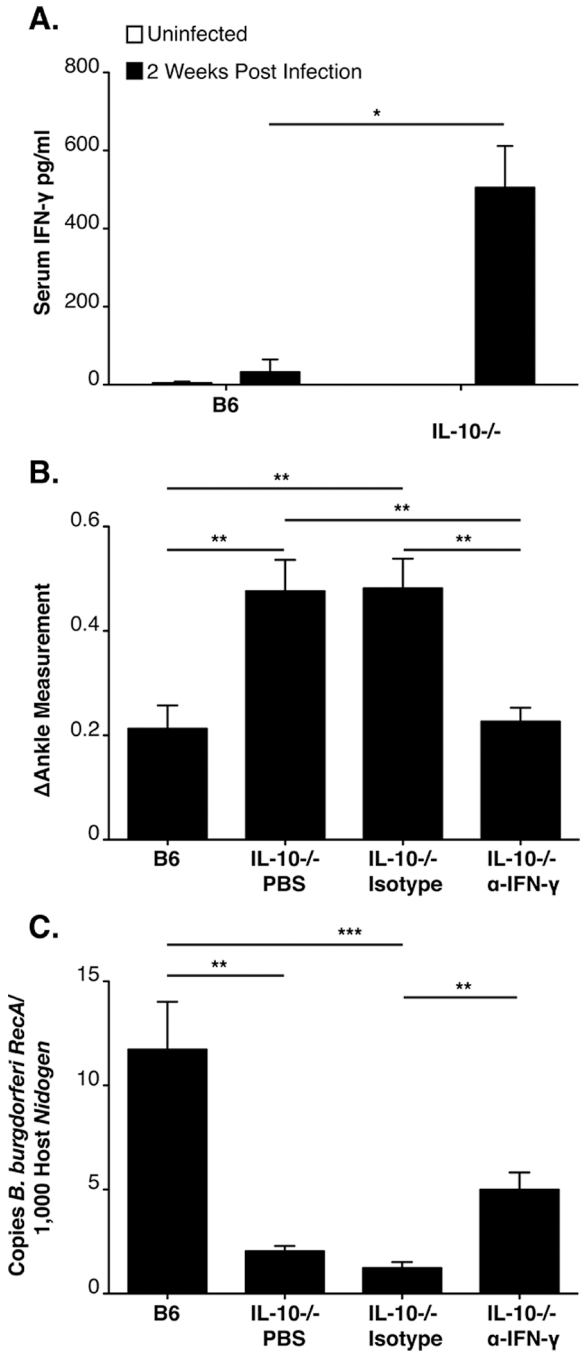

Figure 4. IFN-γ is responsible for the increased arthritis severity in B6 IL-10$^{-/-}$ mice

ELISA of serum IFN-γ at 2 weeks of infection in B6 and B6 IL-10$^{-/-}$ mice (N=5 mice per group (A). Arthritis was assessed in B6 and B6 IL-10$^{-/-}$ mice at 4 weeks of infection (N≥8 mice per group). B6 IL-10$^{-/-}$ mice were injected with PBS, control antibody, or α-IFN-γ over the course of infection. Ankle swelling was used to assess arthritis severity (B). Quantification of joint spirochetes at 4 weeks of infection, using qPCR (C). Statistical analyses were performed as reported in Materials and Methods.

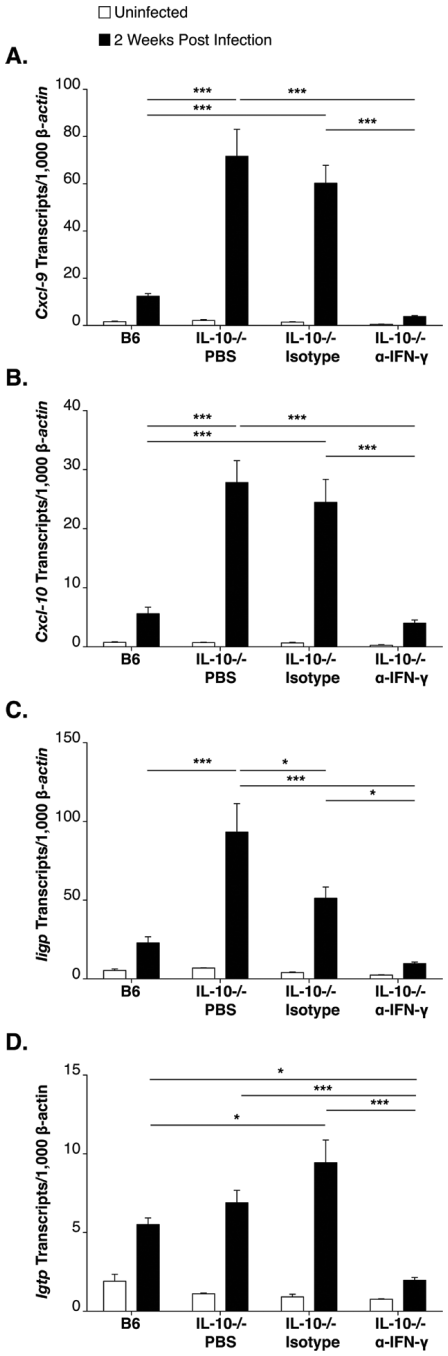

Figure 5. IFN-γ is responsible for the robust expression of interferon-inducible transcripts in B6 IL-10$^{-/-}$ mice

RT-PCR analysis of interferon-inducible transcripts in joint tissue at 14 days of infection in B6 and B6 IL-10$^{-/-}$ mice injected with PBS, isotype control antibody, or α-IFN-γ. N≥6 per group. Expression was normalized to *β-actin* and values represent means ± SEM. Expression of interferon-inducible *CXCL9* (A), *CXCL10* (B) *Iigp* (C) and *Igtp* (D) transcripts are shown. Statistical analyses were performed as reported in Materials and Methods.

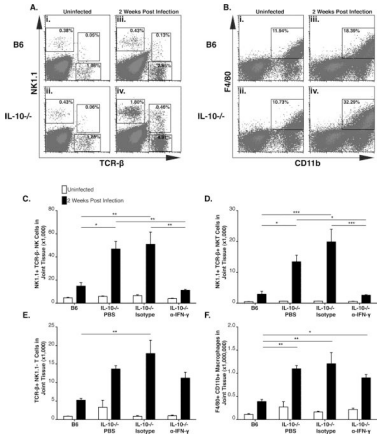

Figure 6. Ankle infiltration by multiple immune cells is regulated by IL-10 in infected B6 mice, and is partially dependent on IFN-γ

Flow cytometry analysis of joint single cell suspensions in B6 and B6 IL-$10^{-/-}$ mice. Data in A and B were acquired from six pooled joints from 3 B6 and 3 B6 IL-$10^{-/-}$ mice. Frequency of NK cells, NKT cells, α/β T cells in uninfected B6 (A-i), uninfected B6 IL-$10^{-/-}$ (A-ii), 2 week infected B6 (A-iii) and 2 week infected B6 IL-$10^{-/-}$ (A-iv) ankle joints. Frequency of macrophages in uninfected B6 (B-i), uninfected B6 IL-$10^{-/-}$ (B-ii), 2 week infected B6 (B-iii), 2 week infected B6 IL-$10^{-/-}$ (B-iv) ankle joints. Infiltration of NK cells (C), NKT cells (D), α/β T cells (E) and macrophages (F) in joint tissue at 14 days of infection in B6 and B6 IL-$10^{-/-}$ mice injected with PBS, isotype control antibody, or α-IFN-γ. N≥3 for each group. Statistical analysis was performed as described in Materials and Methods.

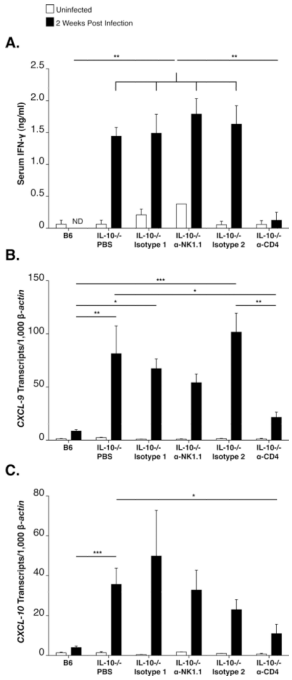

Figure 7. Depletion of CD4^{+} T cells but not NK/ NKT cells reduces expression of interferon inducible transcripts

Analysis of serum IFN-γ and interferon-inducible transcripts in joint tissue at 14 days of infection (N≥7). B6 IL-10$^{-/-}$ mice were injected with PBS, Mouse IgG2a (Isotype 1), α-NK1.1, Rat IgG2b (Isotype 2), or αCD4 during infection. ELISA analysis of serum IFN-γ (A). Expression of *CXCL9* (B) and *CXCL10* (C) in joint tissue was assessed by RT-PCR. Expression was normalized to *β-actin*. Statistical analysis was performed as described in Materials and Methods.

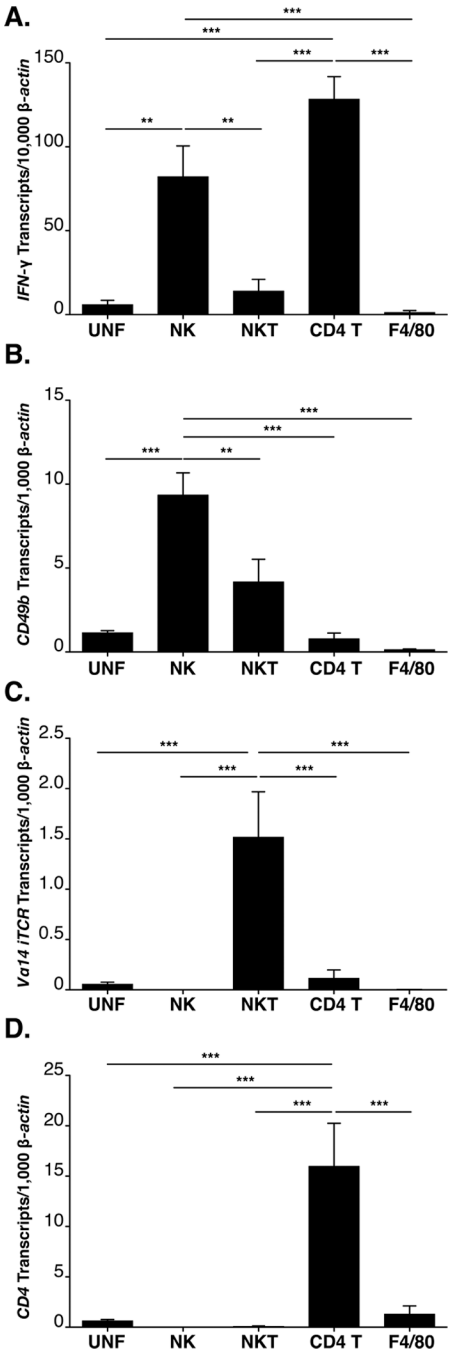

Figure 8. Joint CD4+ T cells and NK cells express high levels of IFN-γ during B. burgdorferi infection

RT-PCR analysis of sorted lineages from infected B6 IL-10$^{-/-}$ joint tissue (N=4). NK cells (NK1.1^{+} TCR-β^{-}, NKT cells (NK1.1^{+} TCR-β^{+}), CD4^{+} T cells (NK1.1^{-}TCR-β^{+} CD4^{+} CD8^{-}) and macrophages (F4/80^{+}) were sorted simultaneously. Expression of IFN-γ transcripts (A) and the transcripts of the definitive lineage markers CD49b (B), Vα14 iTCR (C), CD4 (D), and F4/80 (E) by RT-PCR was used to confirm pure sorted populations. Expression was normalized to *β-actin*. Statistical analysis was performed as described in Materials and Methods.

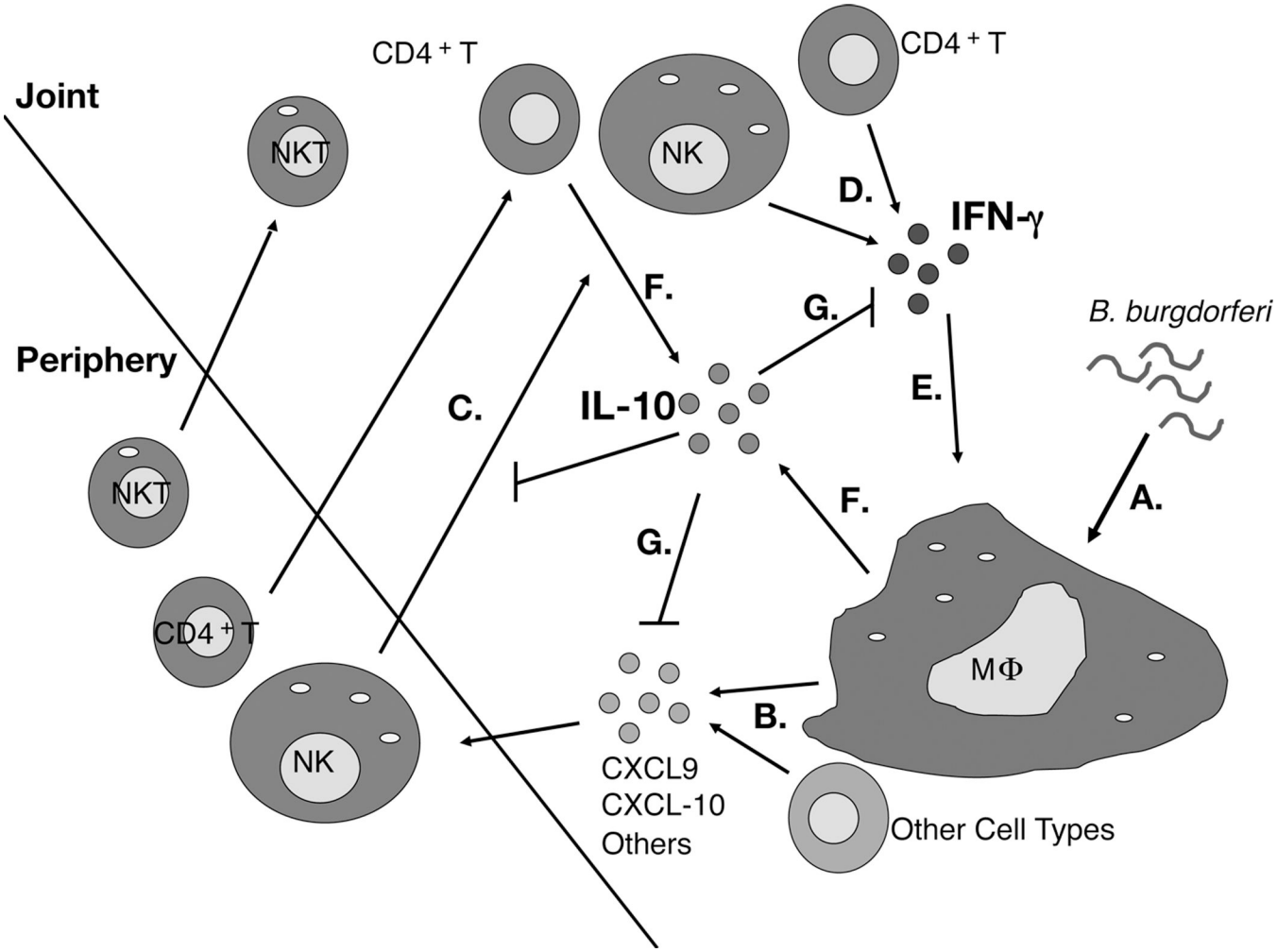

Figure 9. Model of Lyme arthritis development in B6 IL-10$^{-/-}$ mice

B. burgdorferi spirochetes are detected by macrophages and other resident cell types in the joint (A). *B. burgdorferi* stimulated production of CXCL9, CXCL10, and other chemokines is exaggerated in B6 IL-10$^{-/-}$ mice (B). NK cells, NKT cells, CD4^{+} T cells, and other cell types are recruited to the infected joint through the influence of multiple chemokines (C). NK cells and CD4^{+} T cells produce IFN-γ (D). Macrophages and other cell types in the joint are activated by IFN-γ, and produce a second wave of chemokines, including CXCL9 and CXCL10, completing a feedback loop (E). Macrophages and CD4^{+} T cells produce IL-10 (F). IL-10 regulates the expression of IFN-γ, and subsequent production of CXCL9 and CXCL10 (G).

Table I

Comparison of IL-10 (GFP) contributions between macrophages and $CD4^+$ T cells in the joint tissue of *B. burgdorferi* infected *'tiger'* mice.

Cell Type	Day Post Infection	GFP^+ (% of population)[a]	Total GFP^+ Cells (× 1,000)	GFP MFI[b]
$CD4^+$ T cells	11	**44.0±3.1**[**c]	20.2±1.6	**57.3±4.9**[*]
Macrophages	11	6.2±1.1	25.7±6.1	23.9±0.4
$CD4^+$ T cells	14	**24.6±4.0**[*]	4.0±1.0	**37.2±2.5**[*]
Macrophages	14	4.7±1.2	**15.2±3.8**[*]	21.0±0.5

[a] Values represent the mean ± S.E.M

[b] Mean Fluorescence Intensity

[c] Statistical significance (*****) or (******) indicate p values of <0.05 and <0.01 respecively, by student's t-test.

Table II

Assessment of Arthritis by Histopathology in *B. burgdorferi*-infected Joints.[a]

Infected Mouse Strain	Antibody Treatment	Overall Lesion[b]	Neutrophil Infiltration[b]	Mononuclear Infiltration[b]	Sheath Thickening[b]
B6 IL-10$^{-/-}$	PBS (none)	2.88±1.00	2.38±0.46	1.00±0.19	2.38±0.32
B6 IL-10$^{-/-}$	Isotype	2.55±0.77	1.91±0.34	1.27±0.30	2.27±0.24
B6 IL-10$^{-/-}$	α-IFN-γ	**1.50±0.43****	1.17±0.27	**0.33±0.19****	**1.08±0.23****

[a] Assessed at 4 weeks of infection, as described in Materials and Methods

[b] Values represent mean ± S.E.M.

Statistical significance between α-IFN-γ and Isotype is indicated by (**). $p<0.01$ by Mann Whitney U test